Л.Н. Гумилев атындағы Еуразия ұлттық университетінің ХАБАРШЫСЫ.
ISSN: 2616-6836. eISSN: 2663-1296

ФИЗИКА СЕРИЯСЫ/ PHYSICS SERIES / СЕРИЯ ФИЗИКА

IRSTI 29.19.03
Scientific article

https://doi.org/10.32523/2616-6836-2025-152-3-85-99

New manganese hexaboride: stability and mechanical properties

N. Sagatov*[1,2], D. Sagatova[1,3]

[1]*Sobolev Institute of Geology and Mineralogy SB RAS, Novosibirsk, Russian Federation*
[2]*Novosibirsk State University, Novosibirsk, Russian Federation*
[3]*Nikolaev Institute of Inorganic Chemistry SB RAS, Novosibirsk, Russian Federation*

(E-mail: n.e.sagatov@gmail.com)

Abstract. Through *ab initio* evolutionary crystal structure prediction, we have discovered a novel monoclinic phase of manganese hexaboride (MnB_6) with the space group *P2/m.* This new polymorph is energetically favorable over the previously known hexagonal *P6¯m2* structure at pressures below 58 GPa. Although metastable with respect to decomposition into MnB_4 and B, the *P2/m* phase is demonstrated to be dynamically and mechanically stable at ambient pressure, as confirmed by the absence of imaginary phonon modes and the satisfaction of the Born stability criteria. Calculations of the elastic properties reveal that MnB_6-*P2/m* is a hard, brittle material with a high Vickers hardness of 33 GPa, which surpasses that of common industrial ceramics like tungsten carbide and silicon carbide. Its bulk modulus (273 GPa), shear modulus (220 GPa), and Young modulus (519 GPa) indicate superior resistance to elastic deformation. The compound exhibits significant elastic anisotropy, as visualized by the directional dependence of its moduli and hardness. These properties establish the new MnB_6-*P2/m* polymorph as a promising candidate for experimental synthesis and potential application as a hard material.
Keywords: borides, hardness, high pressure, elastic moduli, density functional theory

Introduction

Transition-metal borides have garnered substantial scientific attention due to their remarkable combination of properties, such as superconductivity, magnetism, exceptional hardness, and thermal stability at extreme temperatures [1–6]. The light atomic mass and high bond strength of boron enable the development of extensive covalent networks within transition-metal boride crystals [7]. Progress in computational and synthetic methods has recently enabled the identification and production of numerous borides proposed as superhard candidates, a characteristic attributed to their high valence electron density and strong covalent bonding [8,9]. Notable examples include OsB_2 [10], ReB_2 [2], CrB_2 [11], WB_4 [12], WB_5 [5,13],

Received 31.08.2025. Revised 02.09.2025. Accepted 02.09.2025. Available online 30.09.2025.

[1]*the corresponding author

ZrB_{12} [14], YB_6 [15], ScB_3 [16], ScB_6 [16], and FeB_4 [17]. The measured or predicted hardness of many of these borides exceeds 40 GPa, surpassing that of widely used industrial abrasives and cutting materials such as cemented tungsten carbide (WC, ~20 GPa) [18] and silicon carbide (moissanite, ~22 GPa) [19]. These promising characteristics continue to drive extensive research on transition-metal borides.

Manganese, a magnetic 3d transition metal possessing multiple valence electrons, reacts with boron, an element characterized by its electron deficiency, to produce stable boride compounds. These phases demonstrate a suite of characteristics typical of high-performance multifunctional materials, including exceptional thermal stability (high melting point), superior mechanical strength, and significant resistance to wear. To date, eight manganese–boron compounds are known: Mn_2B, MnB, Mn_3B_4, Mn_2B_3, MnB_2, MnB_3, MnB_4, and MnB_6. Among these manganese borides, MnB_6 is the most B-rich compound. According to the findings of Yuan et al. [20], the MnB6 phase becomes thermodynamically stable at pressures exceeding 127 GPa. This phase, which adopts a *P6¯2m* crystal structure, remains stable up to at least 200 GPa. The crystal structure of MnB_6-*P6¯2m* is characterized by distinctive boron-nitride (BN)-like ribbons that extend along the c-axis. These ribbons are interconnected within the ab-plane via B–B bonds, creating a framework with open channels that house manganese atoms. This phase exhibits favorable mechanical characteristics, including a predicted Vickers hardness of 25 GPa and notable ductility. These properties are a direct consequence of its unique structural arrangement, which is enabled by boron's capacity for diverse and adaptable chemical bonding.

To discover new polymorphs of MnB6 exhibiting promising mechanical properties, we conducted a systematic search for stable crystal structures using density functional theory calculations.

Methodology

All calculations were conducted using density functional theory as implemented in the VASP 5.4.4 software [21, 22]. The exchange–correlation interactions were incorporated through the generalized gradient approximation using the Perdew–Burke–Ernzerhof (PBE) functional. The low-enthalpy structures of MnB_6 were identified through an evolutionary structure search utilizing the USPEX code [23-25]. These variable-composition predictions were conducted for systems containing up to 4 formula units per cell at pressures of 0, 50, 100, 150, and 200 GPa. An initial population of 100 structures was generated, from which the lowest-enthalpy 50% were selected to produce subsequent generations. The evolutionary operations were distributed as follows: 40% heredity, 20% atomic mutation, 10% lattice permutation, and 30% random generation. All structure predictions employed medium-accuracy parameters, including a 450 eV plane-wave energy cutoff, a Monkhorst–Pack k-mesh [26] with a spacing of $2\pi \times 0.07$ Å^{-1}, and Methfessel–Paxton electronic smearing [27] ($\sigma = 0.2$ eV). Following the evolutionary search, the most favorable structures were refined using high-accuracy settings: a 700 eV energy cutoff, a denser k-mesh of $2\pi \times 0.03$ Å^{-1}, and reduced smearing ($\sigma = 0.1$ eV). These selected phases were subjected to full geometry optimization via a conjugate gradient algorithm, with convergence thresholds set to 1.0×10^{-7} eV in energy, 0.01 GPa in stress, and 0.005 eV/Å in atomic forces at

several pressures. The phonon spectra were calculated using the Phonopy program [28] with 2 × 2 × 2 supercell.

To evaluate key mechanical properties such as hardness and fracture toughness, the components of the static elastic stiffness tensor *(C_{ij})* were determined from the linear stress-strain relationship $\sigma_i = C_{ijεj}$. These Cij values were subsequently used to calculate the bulk (B) and shear (G) moduli via the Voigt-Reuss-Hill averaging scheme [29, 30]. For crystalline systems with monoclinic symmetry, the bulk and shear moduli were computed using the following expressions:

$$\begin{cases} B_V = \frac{1}{9}[C_{11} + C_{22} + C_{33} + 2(C_{12} + C_{13} + C_{23}] \\ B_R = \Omega\begin{bmatrix} a(C_{11} + C_{22} - 2C_{12}) + b(2C_{12} - 2C_{11} - 2C_{23}) + c(C_{15} - 2C_{25}) + \\ +d(2C_{12} + 2C_{23} - C_{13} - 2C_{22}) + 2e(C_{25} - C_{15}) + f \end{bmatrix}^{-1} \\ G_V = \frac{1}{15}[C_{11} + C_{22} + C_{33} + 3(C_{44} + C_{55} + C_{66}) - (C_{12} + C_{13} + C_{23})] \\ G_R = 15\left\{\frac{4\begin{bmatrix} a(C_{11} + C_{22} + C_{12}) + b(C_{11} - C_{12} - C_{23}) + c(C_{15} + C_{25}) + \\ +d(C_{22} - C_{12} - C_{23} - C_{13}) + e(C_{15} - C_{25}) + f \end{bmatrix}}{\Delta} + 3\left(\frac{g}{\Omega} + \frac{C_{44} + C_{66}}{C_{44}C_{66} - C_{46}^2}\right)\right\}^{-1} \\ \Delta = C_{13}(C_{12}C_{23} - C_{22}C_{13}) + C_{23}(C_{12}C_{13} - C_{23}C_{11}) + C_{33}(C_{11}C_{22} - C_{12}^2) \\ a = C_{33}C_{55} - C_{35}^2 \\ b = C_{23}C_{55} - C_{25}C_{35} \\ c = C_{13}C_{35} - C_{15}C_{33} \\ d = C_{13}C_{55} - C_{15}C_{35} \\ e = C_{13}C_{25} - C_{15}C_{23} \\ f = C_{11}(C_{22}C_{55} - C_{25}^2) - C_{12}(C_{12}C_{55} - C_{15}C_{25}) + C_{15}(C_{12}C_{25} - C_{15}C_{22}) + C_{25}(C_{23}C_{35} - C_{25}C_{33}) \\ g = C_{11}C_{22}C_{33} - C_{11}C_{23}^2 - C_{22}C_{13}^2 - C_{33}C_{12}^2 + 2C_{12}C_{13}C_{23} \\ \Omega = gC_{55} + 2[C_{15}C_{25}(C_{33}C_{12} - C_{13}C_{23}) + C_{15}C_{35}(C_{22}C_{13} - C_{12}C_{23}) + C_{25}C_{35}(C_{11}C_{23} - C_{12}C_{13})] - \\ -[C_{15}^2(C_{22}C_{33} - C_{23}^2) + C_{25}^2(C_{11}C_{33} - C_{13}^2) + C_{35}^2(C_{11}C_{22} - C_{12}^2)] \\ B = \frac{B_V + B_R}{2} \\ G = \frac{G_V + G_R}{2} \end{cases} \quad (2)$$

Using the obtained bulk and shear moduli, Young's modulus *(E)* and Poisson's ratio *(ν)* could be calculated as follows:

$$E = \frac{9BG}{3B + G}$$
$$\nu = \frac{3B - 2G}{2(3B + G)} \quad (3)$$

To evaluate the Vickers hardness of the predicted MnB_6, the empirical models developed by Chen [31] and Tian [32] were employed:

$$H_V^{Chen} = 2 \cdot (k^2 \cdot G)^{0.585} - 3$$
$$H_V^{Tian} = 0.92 \cdot k^{1.137} \cdot G^{0.708} \quad (4)$$

where *k = G/B.* In this study, the Vickers hardness *(H_V)* was determined by calculating the mean value derived from Equations (4):

$$H_V = \frac{H_V^{Chen} + H_V^{Tian}}{2} \quad (5)$$

Results and discussion

Based on our structure predictions, we identified two low-enthalpy phases of MnB_6. At 100, 150, and 200 GPa, the most stable structure is the *P6m2* phase previously predicted by Yuan et al. [20]. In contrast, at 0 and 50 GPa, we discovered a new, previously unreported phase. This new polymorph of MnB6 crystallizes in the monoclinic *P2/m* space group. There is one inequivalent Mn site. Mn(1) is bonded to four equivalent B(1), four equivalent B(2), and four equivalent B(3) atoms to form a mixture of distorted edge and face-sharing MnB12 cuboctahedra. All Mn(1)-B(1) bond lengths are 2.02 Å. All Mn(1)–B(2) bond lengths are 2.23 Å. All Mn(1)–B(3) bond lengths are 2.32 Å. There are three inequivalent B sites. In the first B site, B(1) is bonded in a 7-coordinate geometry to two equivalent Mn(1), one B(1), two equivalent B(2), and two equivalent B(3) atoms. The B(1)–B(1) bond length is 1.81 Å. Both B(1)–B(2) bond lengths are 1.78 Å. Both B(1)–B(3) bond lengths are 1.79 Å. In the second B site, B(2) is bonded in an 8-coordinate geometry to two equivalent Mn(1), one B(2), two equivalent B(1), and three equivalent B(3) atoms. The B(2)–B(2) bond length is 2.00 Å. There is a spread of B(2)–B(3) bond distances ranging from 1.77–1.92 Å. In the third B site, B(3) is bonded in an 8-coordinate geometry to two equivalent Mn(1), one B(3), two equivalent B(1), and three equivalent B(2) atoms. The B(3)–B(3) bond length is 1.85 Å. The structure can also be characterized as a channel-like open framework of B atoms in which Mn atoms are located. Visualization of the structures and their structural data are presented in Figure 1 and Table 1.

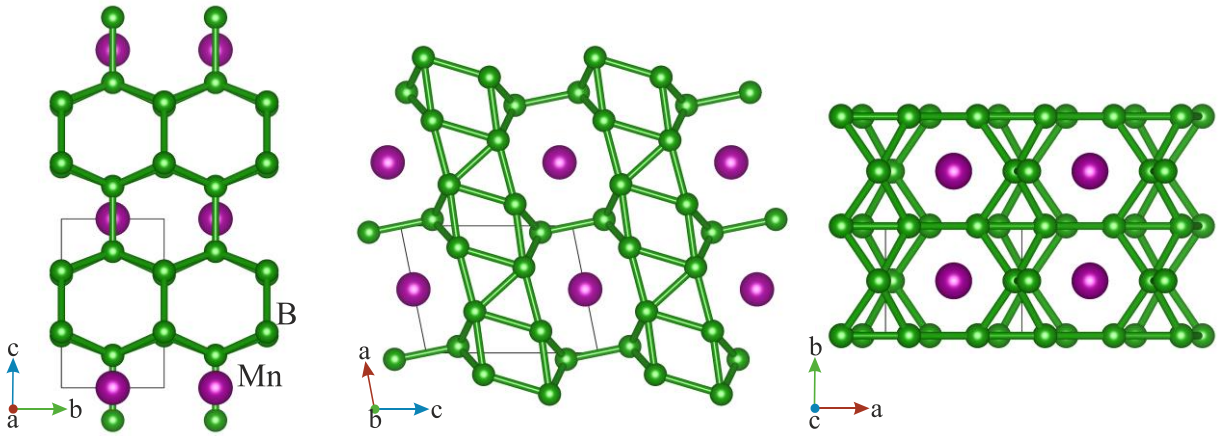

Figure 1. Crystal structure of the predicted MnB_6-*P2/m*

Table 1. Structural data of predicted MnB_6-P2/m at 0 GPa

Space group	Lattice parameters (Å, degree)			Atom	Atomic coordinates		
					x	*y*	*z*
P2/m (#10)	a = 3.618	b = 2.858	c = 4.802	Mn(1)	0.5	0.5	0
	α = 90.00	β = 101.5	γ = 90.00	B(1)	-0.0507	0.5	0.8076
				B(2)	0.1703	0	0.6916
				B(3)	0.6750	0	0.6686

Our enthalpy calculations demonstrate that the newly predicted MnB_6-$P2_1/m$ phase is energetically favorable over the known $P\bar{6}m2$ structure below 58 GPa (Figure 2). Furthermore, spin-polarized calculations indicate that the ground state of this P21/m phase is ferromagnetic. Considering the thermodynamic stability against decomposition ($MnB_6 \rightarrow MnB_4 + 2B$), we can see that the MnB_6 compound stabilizes above 128 GPa in the form of *P6m2* structure (Figure 2), which is in excellent agreement with work of Yuan et al. [20]. Although MnB_6-*P2/m* is inferior in energy to mixture MnB_4 + 2B, it can still be obtained metastably in an experiment if it is dynamically and mechanically stable in calculations.

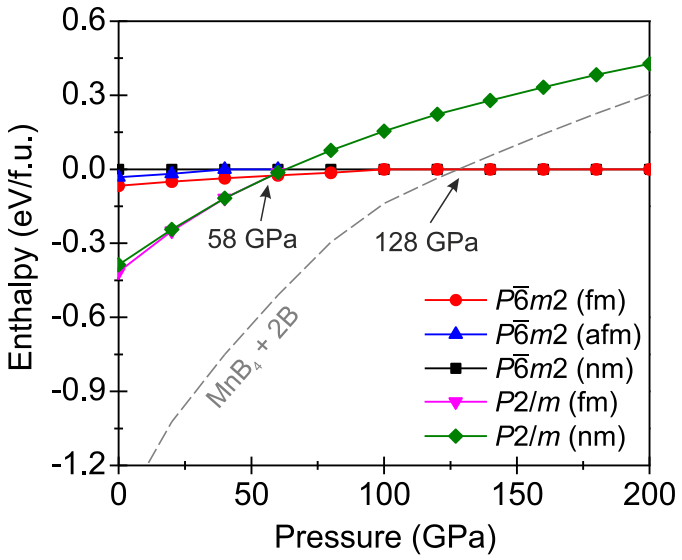

Figure 2. Relative enthalpies of MnB_6 polymorphs as a function of pressure. The gray dashed line indicates the relative enthalpy of MnB_4 + 2B mechanical mixture

To estimate the dynamic stability of MnB_6-*P2/m*, its phonon spectrum at ambient pressure was calculated. The calculated phonon dispersion curves are presented in Figure 3. The absence of imaginary modes in the phonon spectrum is obvious that indicates the dynamic stability of this structure.

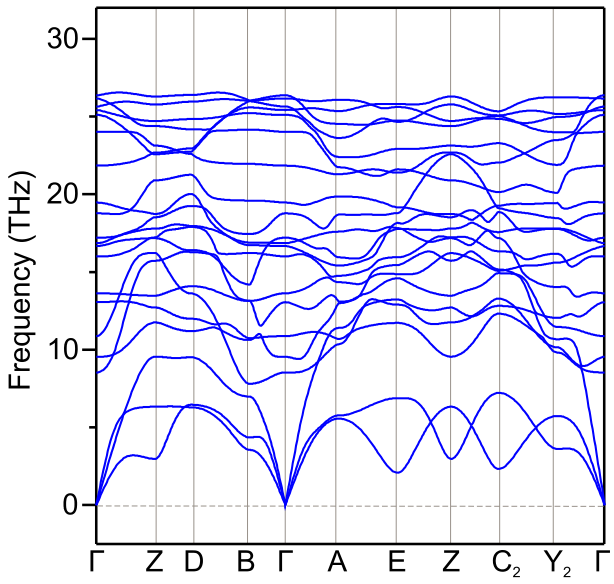

Figure 3. Calculated phonon dispersion curves of MnB6-P2/m

To estimate a mechanical stability of MnB_6-*P2/m,* its second-order elastic stiffness tensor C was calculated using the strain–stress method. The calculated stiffness tensor C (in GPa) is given below:

$$\boldsymbol{C} = \begin{bmatrix} 841 & 99 & 129 & 0 & 13 & 0 \\ 99 & 549 & 102 & 0 & -4 & 0 \\ 129 & 102 & 117.3 & 0 & 16 & 0 \\ 0 & 0 & 0 & 138 & 0 & 25 \\ 13 & -4 & 16 & 0 & 275 & 0 \\ 0 & 0 & 0 & 25 & 0 & 228 \end{bmatrix}$$

The elastic stiffness coefficients (C_{ij}) serve as critical indicators for evaluating the mechanical stability of crystalline phases. For monoclinic systems, the necessary and sufficient conditions for mechanical stability are expressed by the following constraints:

$$\begin{cases} C_{ii} > 0 \ \ (i = 1 - 6) \\ [C_{11} + C_{22} + C_{33} + 2(C_{12} + C_{13} + C_{23})] > 0 \\ (C_{44}C_{66} - C_{46}^2) > 0 \\ (C_{33}C_{55} - C_{35}^2) > 0 \\ (C_{22} + C_{33} - 2C_{23}) > 0 \\ [C_{22}(C_{33}C_{55} - C_{35}^2) + 2C_{23}C_{25}C_{35} - C_{23}^2C_{55} - C_{25}^2C_{33}] > 0 \\ \begin{bmatrix} 2[C_{15}C_{25}(C_{33}C_{12} - C_{13}C_{23}) + C_{15}C_{35}(C_{22}C_{13} - C_{12}C_{23}) + C_{25}C_{35}(C_{11}C_{23} - C_{12}C_{13}) -] \\ -[C_{15}^2(C_{22}C_{33} - C_{23}^2) + C_{25}^2(C_{11}C_{33} - C_{13}^2) + C_{35}^2(C_{11}C_{22} - C_{12}^2)] \\ +(C_{11}C_{22}C_{33} - C_{11}C_{23}^2 - C_{22}C_{13}^2 - C_{33}C_{12}^2 + 2C_{12}C_{13}C_{23})C_{55} \end{bmatrix} > 0 \end{cases}.$$

The calculated C_{ij} values for MnB_6-*P2/m* satisfy the Born criteria, confirming its mechanical stability.

Using the derived C_{ij}, key elastic parameters such as polycrystalline bulk modulus (B), shear modulus (G), Young modulus (E), and Poisson ratio (ν) were determined (Table 2). The calculated polycrystalline bulk modulus of MnB_6-*P2/m* is B = 273 GPa, indicating its resistance to uniform compression is approximately 20% higher than that of silicon carbide (β-SiC, B = 225 GPa [33]) and slightly lower than that of MnB_6-*P6̄m2* (B = 289 GPa [20]). Furthermore, MnB_6-*P2/m* exhibits superior resistance to non-hydrostatic deformation. Its shear modulus (G = 220 GPa) and Young modulus (E = 519 GPa) both exceed those of β-SiC (G = 192 GPa, E = 448 GPa [33]) and almost equal to those of MnB_6-*P6̄m2* (G = 213 GPa, E = 513 GPa [20]). These results suggest the mechanical properties of MnB_6-*P2/m* are superior to those of the widely used SiC, with significantly higher resistance to both shear and axial stresses. Furthermore, its rigidity is comparable to that of the MnB_6-*P6̄m2* polymorph.

Table 2. Calculated polycrystalline elastic moduli, Poisson and B/G ratio of predicted MnB_6 at ambient pressure

Bulk modulus (GPa)	273 GPa
Shear modulus (GPa)	220 GPa
Young modulus (GPa)	519 GPa
Poisson ratio	0.18
B/G	1.24
Vickers hardness (GPa)	33 GPa

The nature of a material, whether it is ductile or brittle, can be determined by its Poisson ratio (ν) and B/G ratio, with established critical values of 0.26 and 1.75, respectively. Values above these thresholds indicate ductility, while those below suggest brittleness. Our calculations for MnB_6-*P2/m* (Table 2) yield values below these critical limits, unequivocally indicating that it exhibits brittle behavior.

While the polycrystalline elastic moduli describe the average elastic response of MnB_6-*P2/m,* a complete mechanical characterization requires an analysis of its directional dependence, or elastic anisotropy. Although dimensionless anisotropy indices offer a preliminary assessment, a comprehensive understanding is best achieved through the three-dimensional visualization of direction-dependent properties. These surfaces quantitatively represent anisotropy by their deviation from spherical symmetry. Figure 4 presents 3D directional plots of the single-crystal elastic moduli and hardness for MnB_6-*P2/m*. Pronounced deviations from spherical symmetry across all surfaces confirm significant elastic anisotropy. The degree of anisotropy varies considerably among the moduli. The bulk modulus exhibits strong directional dependence, varying from 206 GPa along [001] to 429 GPa along [100]. This substantial anisotropy ratio (B[100]/B[001] ≈ 2.1) indicates exceptional orientation-dependent compressibility. In contrast, the shear modulus shows more moderate anisotropy, ranging from 175 GPa along [010] to 253 GPa along [100]. The Young modulus displays the highest degree of elastic anisotropy, with its

magnitude varying dramatically from 360 GPa to 798 GPa depending on the crystallographic direction. Poisson ratio varies from 0.233 to 0.131, demonstrating anisotropy slightly stronger than that of shear modulus.

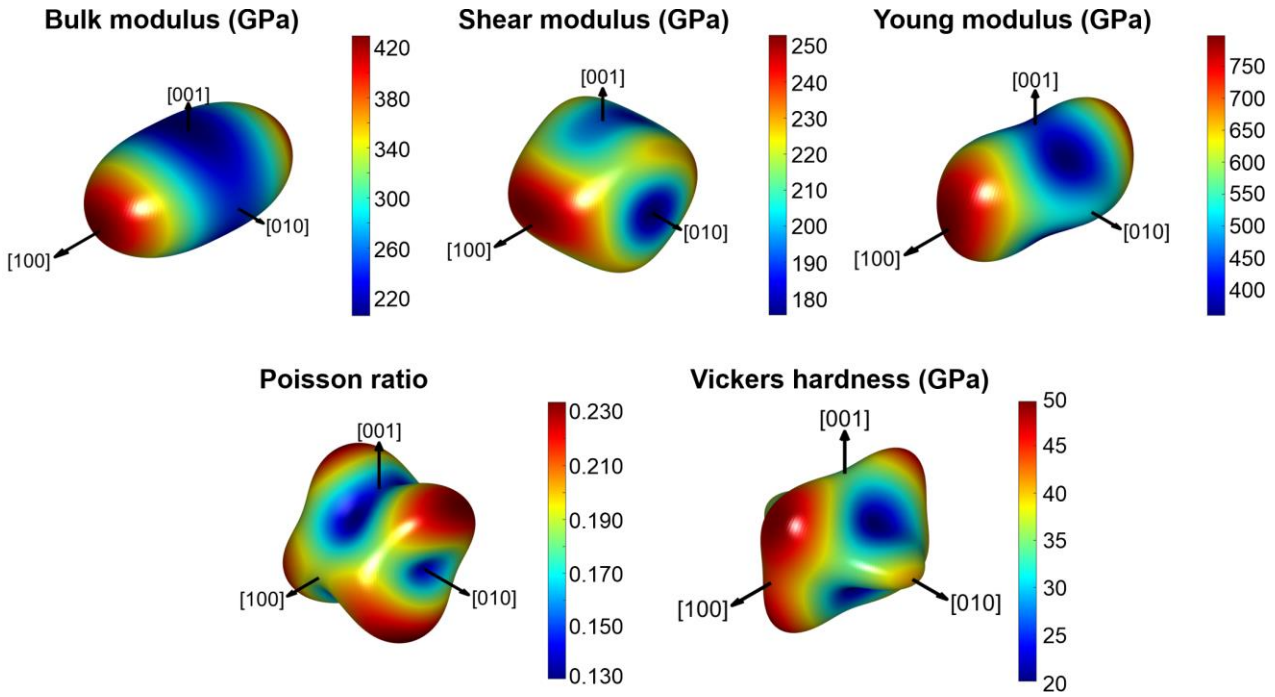

Figure 4. The directional dependence of the bulk modulus, shear modulus, Young modulus, Poisson ratio, and Vickers hardness of MnB_6-*P2/m*

The Vickers hardness of MnB6-P2/m was calculated to determine whether it is classified as hard/superhard material or not. The result of 33 GPa exceeds the minimum threshold for hard materials (HV > 20 GPa) but remains below the criterion for superhard materials (HV > 40 GPa). Thus, MnB6-P2/m is classified as a hard material. The hardness of predicted MnB6-P2/m is higher than known hexagonal polymorph, which hardness equal to 25 GPa [20], and widely used WC (~20 GPa) [18] and SiC (~22 GPa) [19]. The hardness exhibits pronounced anisotropy, as shown in Figure 4, with values ranging from 20.1 GPa to 49.7 GPa-a 2.5-fold variation that highlights its strong directional dependence.

Conclusion

Through crystal structure prediction calculations, we identified a new low-enthalpy polymorph of MnB_6, in addition to the known hexagonal phase. This novel phase, which adopts the monoclinic *P2/m* space group, is energetically favorable over the P$\bar{6}m2$ structure below 58 GPa. Although the *P2/m* polymorph is metastable with respect to the decomposition products across the studied pressure range, it remains a promising candidate for experimental synthesis. This is contingent upon it being dynamically and mechanically stable, as confirmed by our calculations, which would allow it to be obtained metastably. The estimated mechanical properties reveal that MnB_6-*P2/m* has moderate elastic moduli, is brittle, and possesses a high

Vickers hardness of 33 GPa. This hardness surpasses that of widely used industrial materials like cemented tungsten carbide and silicon carbide, firmly classifying MnB_6-*P2/m* as a hard material.

Conflicts of interest

There are no conflicts to declare.

Authorship contribution statement

N. Sagatov – Investigation, Methodology, Analysis, Writing – original draft.

D. Sagatova – Investigation, Methodology, Analysis, Writing – original draft.

References

1. M. Cadeville, Proprietes magnetiques des diborures de manganese et de chrome: MnB2 et CrB2, Journal of Physics and Chemistry of Solids 27, p. 667–670 (1966), DOI: https://doi.org/10.1016/0022-3697(66)90217-4

2. H.-Y. Chung, M.B. Weinberger, J.B. Levine, A. Kavner, J.-M. Yang, S.H. Tolbert, R.B. Kaner, Synthesis of ultra-incompressible superhard rhenium diboride at ambient pressure, Science 316, p. 436–439 (2007), DOI: https://doi.org/10.1126/science.1139322

3. S. Carenco, D. Portehault, C. Boissiere, N. Mezailles, C. Sanchez, Nanoscaled metal borides and phosphides: recent developments and perspectives, Chemical reviews 113, p. 7981–8065 (2013), DOI: https://doi.org/10.1021/cr400020d

4. Q. Li, D. Zhou, W. Zheng, Y. Ma, C. Chen, Anomalous stress response of ultrahard WBn compounds, Physical Review Letters 115, p. 185502 (2015), DOI: https://doi.org/10.1103/PhysRevLett.115.185502

5. A.G. Kvashnin, H.A. Zakaryan, C. Zhao, Y. Duan, Y.A. Kvashnina, C. Xie, H. Dong, A.R. Oganov, New tungsten borides, their stability and outstanding mechanical properties, The Journal of Physical Chemistry Letters 9, p. 3470–3477 (2018), DOI: https://doi.org/10.1021/acs.jpclett.8b01262

6. C. Zhao, Y. Duan, J. Gao, W. Liu, H. Dong, H. Dong, D. Zhang, A.R. Oganov, Unexpected stable phases of tungsten borides, Physical Chemistry Chemical Physics 20, p. 24665–24670 (2018), DOI: https://doi.org/10.1039/C8CP04222E

7. T.P. Fehlner, Molecular models of solid state metal boride structures, Journal of Solid State Chemistry 154, p. 110–113 (2000), DOI: https://doi.org/10.1006/jssc.2000.8820

8. M.T. Yeung, R. Mohammadi, R.B. Kaner, Ultraincompressible, superhard materials, Annual Review of Materials Research 46, p. 465–485 (2016), DOI: https://doi.org/10.1146/annurev-matsci-070115-032148

9. G. Akopov, L.E. Pangilinan, R. Mohammadi, R.B. Kaner, Perspective: Superhard metal borides: A look forward, APL Materials 6(7), p. 070901 (2018), DOI: https://doi.org/10.1063/1.5040763

10. R.W. Cumberland, M.B. Weinberger, J.J. Gilman, S.M. Clark, S.H. Tolbert, R.B. Kaner, Osmium diboride, an ultra-incompressible, hard material, Journal of the American Chemical Society 127, p. 7264–7265 (2005), DOI: https://doi.org/10.1021/ja043806y

11. H. Niu, J. Wang, X.-Q. Chen, D. Li, Y. Li, P. Lazar, R. Podloucky, A.N. Kolmogorov, Structure, bonding, and possible superhardness of CrB4, Physical Review B 85, p. 144116 (2012), DOI: https://doi.org/10.1103/PhysRevB.85.144116

12. R. Mohammadi, A.T. Lech, M. Xie, B.E. Weaver, M.T. Yeung, S.H. Tolbert, R.B. Kaner, Tungsten tetraboride, an inexpensive superhard material, Proceedings of the National Academy of Sciences 108, p. 10958–10962 (2011), DOI: https://doi.org/10.1073/pnas.1102636108

13. A.G. Kvashnin, D.V. Rybkovskiy, V.P. Filonenko, V.I. Bugakov, I.P. Zibrov, V.V. Brazhkin, A.R. Oganov, A.A. Osiptsov, A.Y. Zakirov, WB5−x: Synthesis, properties, and crystal structure–new insights into the long-debated compound, Advanced Science 7, p. 2000775 (2020), DOI: https://doi.org/10.1021/acs.jpcc.5c00183

14. T. Ma, H. Li, X. Zheng, S. Wang, X. Wang, H. Zhao, S. Han, J. Liu, R. Zhang, P. Zhu, Ultrastrong boron frameworks in ZrB12: A highway for electron conducting, Advanced Materials 29, p. 1604003 (2017), DOI: https://doi.org/10.1002/adma.201604003

15. L.-P. Ding, Y.H. Tiandong, P. Shao, Y. Tang, Z.-L. Zhao, H. Lu, Crystal structures, phase stabilities, electronic properties, and hardness of yttrium borides: new insight from first-principles calculations, The Journal of Physical Chemistry Letters 12, p. 5423–5429 (2021), DOI: https://doi.org/10.1021/acs.jpclett.1c01300

16. K. Zhao, Q. Wang, W. Li, Q. Yang, H. Yu, F. Han, H. Liu, S. Zhang, Orthorhombic ScB3 and hexagonal ScB6 with high hardness, Physical Review B 105, p. 094104 (2022), DOI: https://doi.org/10.1103/PhysRevB.105.094104

17. H. Gou, N. Dubrovinskaia, E. Bykova, A.A. Tsirlin, D. Kasinathan, W. Schnelle, A. Richter, M. Merlini, M. Hanfland, A.M. Abakumov, Discovery of a superhard iron tetraboride superconductor, Physical Review Letters 111, p. 157002 (2013), DOI: https://doi.org/10.1103/PhysRevLett.111.157002

18. P. Wang, R. Kumar, E.M. Sankaran, X. Qi, X. Zhang, D. Popov, A.L. Cornelius, B. Li, Y. Zhao, L. Wang, Vanadium diboride (VB2) synthesized at high pressure: elastic, mechanical, electronic, and magnetic properties and thermal stability, Inorganic Chemistry 57, p. 1096–1105 (2018), DOI: https://doi.org/10.1021/acs.inorgchem.7b02550

19. J. Qian, L. Daemen, Y. Zhao, Hardness and fracture toughness of moissanite, Diamond and Related Materials 14, p. 1669–1672 (2005), DOI: https://doi.org/10.1016/j.diamond.2005.06.007

20. X. Yuan, M. Xu, C. Huang, Y. Liang, S. Lin, J. Hao, Y. Li, Pressure-stabilized MnB6 that exhibits high-temperature ferromagnetism and high ductility at ambient pressure, Journal of Materials Chemistry C 10 p. 4365–4371 (2022), DOI: https://doi.org/10.1039/D2TC00508E

21. G. Kresse, J. Furthmüller, Efficiency of ab-initio total energy calculations for metals and semiconductors using a plane-wave basis set, Computational Materials Science 6(1), p. 15-50 (1996), DOI: https://doi.org/10.1016/0927-0256(96)00008-0

22. G. Kresse, D. Joubert, From ultrasoft pseudopotentials to the projector augmented-wave method, Physical Review B 59(3), p. 1758 (1999), DOI: https://doi.org/10.1103/PhysRevB.59.1758

23. A.R. Oganov, C.W. Glass, Crystal structure prediction using ab initio evolutionary techniques: Principles and applications, The Journal of Chemical Physics 124, p. 244704 (2006), DOI: https://doi.org/10.1063/1.2210932

24. A.R. Oganov, A.O. Lyakhov, M. Valle, How evolutionary crystal structure prediction works—and why, Accounts of Chemical Research 44, p. 227–237 (2011), DOI: https://doi.org/10.1021/ar1001318

25. A.O. Lyakhov, A.R. Oganov, H.T. Stokes, Q. Zhu, New developments in evolutionary structure prediction algorithm USPEX, Computer Physics Communications 184, p. 1172–1182 (2013), DOI: https://doi.org/10.1016/j.cpc.2012.12.009

26. H.J. Monkhorst, J.D. Pack, Special points for Brillouin-zone integrations, Physical Review B 13, p. 5188 (1976), DOI: https://doi.org/10.1103/PhysRevB.13.5188

27. M. Methfessel, A.T. Paxton, High-precision sampling for Brillouin-zone integration in metals, Physical Review B 40, p. 3616 (1989), DOI: https://doi.org/10.1103/PhysRevB.40.3616

28. A. Togo, I. Tanaka, First principles phonon calculations in materials science, Scripta Materialia 108, p. 1–5 (2015), DOI: https://doi.org/10.1016/j.scriptamat.2015.07.021

29. R. Hill, The elastic behaviour of a crystalline aggregate, Proceedings of the Physical Society. Section A 65, p. 349 (1952), DOI: https://doi.org/10.1088/0370-1298/65/5/307

30. R. Hill, Elastic properties of reinforced solids: some theoretical principles, Journal of the Mechanics and Physics of Solids 11, p. 357–372 (1963), DOI: https://doi.org/10.1016/0022-5096(63)90036-X

31. X.-Q. Chen, H. Niu, D. Li, Y. Li, Modeling hardness of polycrystalline materials and bulk metallic glasses, Intermetallics 19, p. 1275–1281 (2011), DOI: https://doi.org/10.1016/j.intermet.2011.03.026

32. Y. Tian, B. Xu, Z. Zhao, Microscopic theory of hardness and design of novel superhard crystals, International Journal of Refractory Metals and Hard Materials 33, p. 93–106 (2012), DOI: https://doi.org/10.1016/j.ijrmhm.2012.02.021

33. R.D. Carnahan, Elastic properties of silicon carbide, Journal of the American Ceramic Society 51(4), p. 223-224 (1968), DOI: https://doi.org/10.1111/j.1151-2916.1968.tb11877.x

Н. Сағатов[1,2], Д. Сағатова[1,3]

[1]В.С. Соболев ат. геология және минералогия институты РҒА СТ, Новосибирск, Ресей Федерациясы

[2]Новосибирск мемлекеттік университеті, Новосибирск, Ресей Федерациясы.

[3]А.В. Николаев ат. бейорганикалық химия институты РҒА СТ, Новосибирск, Ресей Федерациясы (E-mail: n.e.sagatov@gmail.com)

Жаңа марганец гексабориді: тұрақтылық және механикалық қасиеттер

Аңдатпа. *Ab initio* эволюциялық кристалдық құрылымды болжауды пайдалана отырып, біз *P2/m* кеңістік тобымен марганец гексаборидінің (MnB_6) жаңа моноклиндық фазасын аштық. Бұл жаңа полиморф 58 ГПа төмен қысымда бұрын белгілі гексагональдық *Pб̄m2* құрылымымен салыстырғанда энергетикалық жағынан қолайлы. *P2/m* фазасы MnB_4 және B-ге ыдырауға қатысты метатұрақты болғанымен, оның қоршаған орта қысымында динамикалық және механикалық тұрақтылығы көрсетілген, бұл ойдан шығарылған фонон модтардың жоқтығымен және Борн тұрақтылық критерийлерінің қанағаттандырылуымен дәлелденеді. Серпімді есептеулер MnB_6-*P2/m* қатты, сынғыш материал екенін көрсетеді, жоғары Викерс қаттылығы 33 ГПа, ол вольфрам карбиді және кремний карбиді сияқты қарапайым өнеркәсіптік керамикадан жоғары. Көлемдік модуль (273 ГПа), ығысу модулі (220 ГПа) және Янг модулі (519 ГПа) серпімді деформацияға тамаша қарсылықты көрсетеді. Қосылыс айтарлықтай серпімді анизотропияны көрсетеді, бұл оның модульдері мен қаттылығының бағытталған тәуелділігімен дәлелденеді. Бұл қасиеттер жаңа MnB_6-*P2/m* полиморфты тәжірибелік синтез және қатты материал ретінде әлеуетті қолдану үшін перспективалы үміткер етеді.

Түйін сөздер: боридтер, қаттылық, жоғары қысым, серпімділік модульдері, тығыздық функционалдық теориясы

Н. Сагатов[1,2], Д. Сагатова[1,3]

[1]Институт геологии и минералогии им В.С. Соболева СО РАН, Новосибирск, Российская Федерация

[2]Новосибирский государственный университет, Новосибирск, Российская Федерация

[3]Институт неорганической химии им. А.В. Николаева СО РАН, Новосибирск, Российская Федерация

(E-mail: n.e.sagatov@gmail.com)

Новый гексаборид марганца: стабильность и механические свойства

Аннотация. С помощью *ab initio* эволюционных предсказаний кристаллических структур мы обнаружили новую моноклинную фазу гексаборида марганца (MnB_6) с пространственной группой *P2/m*. Этот новый полиморф энергетически выгоден по сравнению с ранее известной гексагональной структурой $P\bar{6}m2$ при давлениях ниже 58 ГПа. Хотя фаза *P2/m* метастабильна относительно распада на MnB_4 и B, продемонстрировано, что она динамически и механически стабильна при давлении окружающей среды, что подтверждается отсутствием мнимых фононных мод и удовлетворением критериям устойчивости Борна. Расчеты упругих свойств показывают, что MnB_6-*P2/m* является твердым, хрупким материалом с высокой твердостью по Виккерсу 33 ГПа, что превосходит твердость обычных промышленных керамик, таких, как карбид вольфрама и карбид кремния. Модуль объёмной упругости (273 ГПа), модуль сдвига (220 ГПа) и модуль Юнга (519 ГПа) указывают на превосходную устойчивость к упругой деформации. Соединение обладает значительной упругой анизотропией, что подтверждается направленной зависимостью его модулей и твёрдости. Эти свойства делают новый полиморф MnB_6-*P2/m* перспективным кандидатом для экспериментального синтеза и потенциального применения в качестве твёрдого материала.

Ключевые слова: бориды, твердость, высокое давление, модули упругости, теория функционала плотности

References

1. M. Cadeville, Proprietes magnetiques des diborures de manganese et de chrome: MnB2 et CrB2, Journal of Physics and Chemistry of Solids 27, p. 667–670 (1966), DOI: https://doi.org/10.1016/0022-3697(66)90217-4

2. H.-Y. Chung, M.B. Weinberger, J.B. Levine, A. Kavner, J.-M. Yang, S.H. Tolbert, R.B. Kaner, Synthesis of ultra-incompressible superhard rhenium diboride at ambient pressure, Science 316, p. 436–439 (2007), DOI: https://doi.org/10.1126/science.1139322

3. S. Carenco, D. Portehault, C. Boissiere, N. Mezailles, C. Sanchez, Nanoscaled metal borides and phosphides: recent developments and perspectives, Chemical reviews 113, p. 7981–8065 (2013), DOI: https://doi.org/10.1021/cr400020d

4. Q. Li, D. Zhou, W. Zheng, Y. Ma, C. Chen, Anomalous stress response of ultrahard WBn compounds, Physical Review Letters 115, p. 185502 (2015), DOI: https://doi.org/10.1103/PhysRevLett.115.185502

5. A.G. Kvashnin, H.A. Zakaryan, C. Zhao, Y. Duan, Y.A. Kvashnina, C. Xie, H. Dong, A.R. Oganov, New tungsten borides, their stability and outstanding mechanical properties, The Journal of Physical Chemistry Letters 9, p. 3470–3477 (2018), DOI: https://doi.org/10.1021/acs.jpclett.8b01262

6. C. Zhao, Y. Duan, J. Gao, W. Liu, H. Dong, H. Dong, D. Zhang, A.R. Oganov, Unexpected stable phases of tungsten borides, Physical Chemistry Chemical Physics 20, p. 24665–24670 (2018), DOI: https://doi.org/10.1039/C8CP04222E

7. T.P. Fehlner, Molecular models of solid state metal boride structures, Journal of Solid State Chemistry 154, p. 110–113 (2000), DOI: https://doi.org/10.1006/jssc.2000.8820

8. M.T. Yeung, R. Mohammadi, R.B. Kaner, Ultraincompressible, superhard materials, Annual Review of Materials Research 46, p. 465–485 (2016), DOI: https://doi.org/10.1146/annurev-matsci-070115-032148

9. G. Akopov, L.E. Pangilinan, R. Mohammadi, R.B. Kaner, Perspective: Superhard metal borides: A look forward, APL Materials 6(7), p. 070901 (2018), DOI: https://doi.org/10.1063/1.5040763

10. R.W. Cumberland, M.B. Weinberger, J.J. Gilman, S.M. Clark, S.H. Tolbert, R.B. Kaner, Osmium diboride, an ultra-incompressible, hard material, Journal of the American Chemical Society 127, p. 7264–7265 (2005), DOI: https://doi.org/10.1021/ja043806y

11. H. Niu, J. Wang, X.-Q. Chen, D. Li, Y. Li, P. Lazar, R. Podloucky, A.N. Kolmogorov, Structure, bonding, and possible superhardness of CrB4, Physical Review B 85, p. 144116 (2012), DOI: https://doi.org/10.1103/PhysRevB.85.144116

12. R. Mohammadi, A.T. Lech, M. Xie, B.E. Weaver, M.T. Yeung, S.H. Tolbert, R.B. Kaner, Tungsten tetraboride, an inexpensive superhard material, Proceedings of the National Academy of Sciences 108, p. 10958–10962 (2011), DOI: https://doi.org/10.1073/pnas.1102636108

13. A.G. Kvashnin, D.V. Rybkovskiy, V.P. Filonenko, V.I. Bugakov, I.P. Zibrov, V.V. Brazhkin, A.R. Oganov, A.A. Osiptsov, A.Y. Zakirov, WB5−x: Synthesis, properties, and crystal structure–new insights into the long-debated compound, Advanced Science 7, p. 2000775 (2020), DOI: https://doi.org/10.1021/acs.jpcc.5c00183

14. T. Ma, H. Li, X. Zheng, S. Wang, X. Wang, H. Zhao, S. Han, J. Liu, R. Zhang, P. Zhu, Ultrastrong boron frameworks in ZrB12: A highway for electron conducting, Advanced Materials 29, p. 1604003 (2017), DOI: https://doi.org/10.1002/adma.201604003

15. L.-P. Ding, Y.H. Tiandong, P. Shao, Y. Tang, Z.-L. Zhao, H. Lu, Crystal structures, phase stabilities, electronic properties, and hardness of yttrium borides: new insight from first-principles calculations, The Journal of Physical Chemistry Letters 12, p. 5423–5429 (2021), DOI: https://doi.org/10.1021/acs.jpclett.1c01300

16. K. Zhao, Q. Wang, W. Li, Q. Yang, H. Yu, F. Han, H. Liu, S. Zhang, Orthorhombic ScB3 and hexagonal ScB6 with high hardness, Physical Review B 105, p. 094104 (2022), DOI: https://doi.org/10.1103/PhysRevB.105.094104

17. H. Gou, N. Dubrovinskaia, E. Bykova, A.A. Tsirlin, D. Kasinathan, W. Schnelle, A. Richter, M. Merlini, M. Hanfland, A.M. Abakumov, Discovery of a superhard iron tetraboride superconductor, Physical Review Letters 111, p. 157002 (2013), DOI: https://doi.org/10.1103/PhysRevLett.111.157002

18. P. Wang, R. Kumar, E.M. Sankaran, X. Qi, X. Zhang, D. Popov, A.L. Cornelius, B. Li, Y. Zhao, L. Wang, Vanadium diboride (VB2) synthesized at high pressure: elastic, mechanical, electronic, and magnetic properties and thermal stability, Inorganic Chemistry 57, p. 1096–1105 (2018), DOI: https://doi.org/10.1021/acs.inorgchem.7b02550

19. J. Qian, L. Daemen, Y. Zhao, Hardness and fracture toughness of moissanite, Diamond and Related Materials 14, p. 1669–1672 (2005), DOI: https://doi.org/10.1016/j.diamond.2005.06.007

20. X. Yuan, M. Xu, C. Huang, Y. Liang, S. Lin, J. Hao, Y. Li, Pressure-stabilized MnB6 that exhibits high-temperature ferromagnetism and high ductility at ambient pressure, Journal of Materials Chemistry C 10 p. 4365–4371 (2022), DOI: https://doi.org/10.1039/D2TC00508E

21. G. Kresse, J. Furthmüller, Efficiency of ab-initio total energy calculations for metals and semiconductors using a plane-wave basis set, Computational Materials Science 6(1), p. 15-50 (1996), DOI: https://doi.org/10.1016/0927-0256(96)00008-0

22. G. Kresse, D. Joubert, From ultrasoft pseudopotentials to the projector augmented-wave method, Physical Review B 59(3), p. 1758 (1999), DOI: https://doi.org/10.1103/PhysRevB.59.1758

23. A.R. Oganov, C.W. Glass, Crystal structure prediction using ab initio evolutionary techniques: Principles and applications, The Journal of Chemical Physics 124, p. 244704 (2006), DOI: https://doi.org/10.1063/1.2210932

24. A.R. Oganov, A.O. Lyakhov, M. Valle, How evolutionary crystal structure prediction works—and why, Accounts of Chemical Research 44, p. 227–237 (2011), DOI: https://doi.org/10.1021/ar1001318

25. A.O. Lyakhov, A.R. Oganov, H.T. Stokes, Q. Zhu, New developments in evolutionary structure prediction algorithm USPEX, Computer Physics Communications 184, p. 1172–1182 (2013), DOI: https://doi.org/10.1016/j.cpc.2012.12.009

26. H.J. Monkhorst, J.D. Pack, Special points for Brillouin-zone integrations, Physical Review B 13, p. 5188 (1976), DOI: https://doi.org/10.1103/PhysRevB.13.5188

27. M. Methfessel, A.T. Paxton, High-precision sampling for Brillouin-zone integration in metals, Physical Review B 40, p. 3616 (1989), DOI: https://doi.org/10.1103/PhysRevB.40.3616

28. A. Togo, I. Tanaka, First principles phonon calculations in materials science, Scripta Materialia 108, p. 1–5 (2015), DOI: https://doi.org/10.1016/j.scriptamat.2015.07.021

29. R. Hill, The elastic behaviour of a crystalline aggregate, Proceedings of the Physical Society. Section A 65, p. 349 (1952), DOI: https://doi.org/10.1088/0370-1298/65/5/307

30. R. Hill, Elastic properties of reinforced solids: some theoretical principles, Journal of the Mechanics and Physics of Solids 11, p. 357–372 (1963), DOI: https://doi.org/10.1016/0022-5096(63)90036-X

31. X.-Q. Chen, H. Niu, D. Li, Y. Li, Modeling hardness of polycrystalline materials and bulk metallic glasses, Intermetallics 19, p. 1275–1281 (2011), DOI: https://doi.org/10.1016/j.intermet.2011.03.026

32. Y. Tian, B. Xu, Z. Zhao, Microscopic theory of hardness and design of novel superhard crystals, International Journal of Refractory Metals and Hard Materials 33, p. 93–106 (2012), DOI: https://doi.org/10.1016/j.ijrmhm.2012.02.021

33. R.D. Carnahan, Elastic properties of silicon carbide, Journal of the American Ceramic Society 51(4), p. 223-224 (1968), DOI: https://doi.org/10.1111/j.1151-2916.1968.tb11877.x

Information about the authors:

Sagatov N. **–** corresponding author, candidate of physical and mathematical sciences, researcher of the Sobolev Institute of geology and mineralogy SB RAS, prospect akademika Koptyuga, 3, Novosibirsk, Russian Federation.

Sagatova D. **–** candidate of geological and mineralogical sciences, researcher of the Sobolev Institute of geology and mineralogy SB RAS, prospect akademika Koptyuga, 3, Novosibirsk, Russian Federation.

Сағатов Н. **–** хат-хабар авторы, физика-математика ғылымдарының кандидаты, РҒА СТ В.С. Соболев атындағы Геология және Минералогия институтының ғылыми қызметкері, академик Коптюг даңғылы, 3, Новосибирск, Ресей Федерациясы.

Сағатова Д. **–** геология-минералогия ғылымдарының кандидаты, РҒА СТ В.С. Соболев атындағы Геология және Минералогия институтының ғылыми қызметкері, академик Коптюг даңғылы, 3, Новосибирск, Ресей Федерациясы.

Сагатов Н. **–** автор для корреспонденции, кандидат физико-математических наук, научный сотрудник Института геологии и минералогии им В.С. Соболева СО РАН, проспект академика Коптюга, 3, Новосибирск, Российская Федерация.

Сагатова Д. – кандидат геолого-минералогических наук, научный сотрудник Института геологии и минералогии им В.С. Соболева СО РАН, проспект академика Коптюга, 3, Новосибирск, Российская Федерация.